Thorium effect on the oxidation of uranium: Photoelectron spectroscopy (XPS/UPS) and cyclic voltammetry (CV) investigation on (U1 − xThx)O2 (x = 0 to 1) thin films

Cakir, P.; Eloirdi, R; Huber, F.; Konings, R. J.M.; Gouder, T

DOI
10.1016/j.apsusc.2016.10.010

Publication date
2017

Document Version
Final published version

Published in
Applied Surface Science

Applied Surface Science 393 (2017) 204–211

Contents lists available at ScienceDirect

Applied Surface Science

journal homepage: www.elsevier.com/locate/apsusc

Full Length Article

Thorium effect on the oxidation of uranium: Photoelectron spectroscopy (XPS/UPS) and cyclic voltammetry (CV) investigation on $(U_{1-x}Th_x)O_2$ (x = 0 to 1) thin films

P. Cakir[a,b,*], R. Eloirdi[a], F. Huber[a], R.J.M. Konings[a,b], T. Gouder[a]

[a] European Commission, Joint Research Centre, P.O. Box 2340, D-76125, Karlsruhe, Germany
[b] Department of Radiation Science and Technology, Delft University of Technology, Mekelweg 15, 2629, JB Delft, The Netherlands

ARTICLE INFO

Article history:
Received 17 August 2016
Received in revised form
27 September 2016
Accepted 3 October 2016
Available online 4 October 2016

Keywords:
Thin film
Mixed oxide
Electrochemistry
Corrosion
Actinide oxide

ABSTRACT

Thin films of $U_{1-x}Th_xO_2$ (x = 0 to 1) have been deposited via reactive DC sputter technique and characterized by X-ray/Ultra-violet Photoelectron Spectroscopy (XPS/UPS), X-ray Powder Diffractometer (XRD) and Cyclic Voltammetry (CV) in order to understand the effect of Thorium on the oxidation mechanism. During the deposition, the competition between uranium and thorium for oxidation showed that thorium has a much higher affinity for oxygen. Deposition conditions, time and temperature were also the subject of this study, to look at the homogeneity and the stability of the films. While core level and valence band spectra were not altered by the time of deposition, temperature was affecting the oxidation state of uranium and the valence band due to the mobility increase of oxygen through the film. X-ray diffraction patterns, core level spectra obtained for $U_{1-x}Th_xO_2$ versus the composition showed that lattice parameters follow the Vegard's law and together with the binding energies of U-*4f* and Th-*4f* are in good agreement with literature data obtained on bulk compounds. To study the effect of thorium on the oxidation of $U_{1-x}Th_xO_2$ films, we used CV experiments at neutral pH of a NaCl solution in contact with air. The results indicated that thorium has an effect on the uranium oxidation as demonstrated by the decrease of the current of the oxidation peak of uranium. XPS measurements made before and after the CV, showed a relative enrichment of thorium at the extent of uranium at the surface supporting the formation at a longer term of a thorium protective layer at the surface of uranium-thorium mixed oxide.

1. Introduction

Thorium-Uranium mixed oxides are interesting nuclear fuel materials. Compared to uranium- plutonium mixed oxide, the higher thermal stability and melting temperature results in a larger margin to melting [1]. The use of Thorium-Uranium mixed oxide results in the production of smaller quantities of Transuranium elements [2].

During the geological storage of used nuclear fuel, the radionuclides embedded in the uranium fuel matrix, which are produced during the reactor irradiation, can be released via the dissolution of the fuel matrix. Uranium has two stable oxidation states, (IV) and (VI), and several mixed valence phases (i.e. U_3O_7, U_4O_9, U_3O_8). The solubility of uranium increases several magnitudes as the oxidation state increases from U (IV) to U (VI) in the matrix [3]. On the other hand, ThO_2 is chemically stable, having one oxidation state (IV), and its dissolution is reported to be extremely difficult [4].

Since the first contact of the material with the environment happens on the surface, our interest is to observe changes and the evolution of the oxide layer forming at the interface. In this work, thin films of (U, Th) mixed oxides formed by sputter deposition technique [5] are used instead of using bulk material [6–9]. The use of thin films to simulate the surface of bulk compounds results in a high flexibility for compositional changes (O/(U + Th) or U/Th ratios). Moreover, it allows deposition of layers of different thickness onto variable substrates, with different microstructure when changing the temperature and gas pressure during the deposition.

Materials such as uranium – thorium oxides, are difficult to study by photoelectron spectroscopy [10], which is due to their semiconductor properties as a result of which the flow of current cannot be achieved properly along the bulk sample thickness. This aspect can be limited or avoided by the use of thin films because the low thickness results in a low resistance and the voltage drop can be neglected [11,12].

* Corresponding author at: European Commission, Joint Research Centre, P.O. Box 2340, D-76125, Karlsruhe, Germany.
E-mail address: pelincakir@outlook.com (P. Cakir).

http://dx.doi.org/10.1016/j.apsusc.2016.10.010

The main goal of this study is to understand the effect of the stable tetravalent actinide Th(IV) onto uranium dioxide and to follow the electronic structure, oxidation state and redox reactions on the surface.

The paper is divided into three sections. The first part investigates the relative oxygen affinity between uranium and thorium, by bringing them into competition. The second part examines the effect of high temperature and low temperature deposition on the surface properties such as oxygen diffusion and atomic segregation. Also in this part, we compare $U_{1-x}Th_xO_2$ (x = 0 to 1) thin films to bulk materials to confirm their use as model, by analysing their electronic structure and lattice parameters versus their composition. The third part consists of electrochemical studies on $U_{1-x}Th_xO_2$ films (X = 0 to 1). Electrochemistry, especially cyclic voltammetry (CV) of UO_2 samples has been intensively employed [13–18] however to the best of our knowledge, there has been no CV record on uranium-thorium mixed oxides, probably due to the semiconductor properties. The objective of the current CV studies is to examine the oxidation of $U_{1-x}Th_xO_2$ before and after the CV using XPS, looking at the composition and the oxidation state.

2. Experimental

The thin films of $U_{1-x}Th_xO_2$ (x = 0 to 1) were prepared in-situ by direct current reactive co-sputtering from thorium and uranium metal targets in a gas mixture of Ar (6N) and O_2 (6N). The oxygen concentration in the films was adjusted by changing the O_2 partial pressure (10^{-8} mbar–6×10^{-6} mbar), while the Ar partial pressure was maintained at 5×10^{-7} mbar. The composition of the films is controlled by changing the respective target voltages for U and Th target. The thin films were deposited onto silicon wafer (111) substrates, which were cleaned by Ar ion sputtering (4 keV) for 1 min. The plasma in the diode source was maintained by injection of electrons of 50–100 eV energy (triode setup), allowing working at low Ar pressure in absence of stabilizing magnetic fields. After deposition, the thin films were transferred to the XPS-UPS analysis chamber without exposing them to air.

Photoelectron spectroscopy data were recorded using a hemispherical analyser from Omicron (EA 125 U5). The spectra were taken using Mg Kα (1253.6 eV) radiation with an approximate energy resolution of 1 eV. UPS measurements were made using He*II* (40.81 eV) excitation radiation produced by a high intensity windowless UV rare gas discharge source (SPECS UVS 300). The total resolution in UPS was 0.1–0.05 eV for the high resolution scans. The background pressure in the analysis chamber was 2×10^{-10} mbar. The spectrometer was calibrated by using Au-$4f_{7/2}$ line of metal to give a value at 83.9 eV BE and Cu-$2p_{3/2}$ line of metal at 932.7 eV BE for XPS, and on He*I* and He*II* Fermi-edges for UPS. Photoemission spectra were taken at room temperature. Quantification of the spectra was done using CasaXPS software (version 2.3.13Dev50). As Relative Sensitivity Factors, Scofield cross-sections for Mg-Kα radiation [19] were taken. An example of peaks deconvolution with the CasaXPS software is reported in Fig. 1.

For the electrochemical study, a standard 3-electrode setup was used with a working electrode composed of $U_{1-x}Th_xO_2$ (x = 0.00, 0.10, 0.44, 0.84, 1.00) thin films deposited onto gold foil surface; the reference electrode was an Ag/AgCl (3 M KCl) electrode and a Pt wire as counter electrode. Gold foils were first cleaned with Ethanol/1N H_2SO_4/H_2O then heated till 300 °C under ultra-high vacuum (UHV). As adhesion layer, an interface composed of a (U,Th) metal layer was deposited at 300 °C between the gold foil and the $U_{1-x}Th_xO_2$ film. All potential values in this paper are versus Ag/AgCl. The measurements were carried out with a stationary electrode in an unstirred solution. The electrolyte was a 0.01 M NaCl solution at neutral pH in contact with air. Experiments were carried out at room temperature (22 ± 3 °C) in a closed Teflon electrochemical cell with an electrolyte volume of 3 ml. Applied potentials were not corrected for voltage drop because of the negligible electrode resistance of the film electrodes [11]. Before the scans, the electrodes were preconditioned at the most cathodic potential for 5 min to reduce any higher oxides formed during the transportation. The cyclovoltammetry (CV) measurements were recorded in potential sweep cycles in a first series (15 cycles) from −1.000 $V_{Ag/AgCl}$ up to +0.600 $V_{Ag/AgCl}$, and back to −1.000 $V_{Ag/AgCl}$ and then in a second series (15 cycles) from −1 $V_{Ag/AgCl}$ to 0.8 $V_{Ag/AgCl}$ at a scan rate of 0.010 V s^{-1}. Ultrapure water from a MilliQ-system (>18 MΩ) was used. Chemicals were all p.a. grade (Merck, Darmstadt).

The X-ray diffraction analyses were made on a conventional Phillips PW3830 powder diffractometer with a Cu X-ray tube (40 kV, 30 mA, Kα1 = 0.1540560 nm). Films of about 360 nm (1 Å/s) thicknesses were deposited at 100 °C on a Si (111) wafer. The patterns were recorded at room temperature in a step scan mode over a 2Θ range of [10–100]°, with a step size of 0.01° and a count time of 5 s per step.

Table 1
Binding energy of $4f_{5/2}$ core level peak for Th metal, U metal, ThO_2 and UO_2.

Substance	$4f_{5/2}$ (eV)	satellite
Th metal	342.3 [20,43]	–
U metal	388.40 [44]	–
ThO_2	346.8 [20,45]	7.3
UO_2	390.95 [11,46]	6.7

3. Results and discussion

3.1. Relative oxygen affinity

To measure the relative oxygen affinity of thorium and uranium, a series of thin films were deposited successively by increasing the oxygen partial pressure with a low increment and analysing them in-situ by XPS. The U-*4f* and Th-*4f* core level spectra enable to investigate the oxidation of uranium and thorium through their binding energy (BE) peak, their shape and their satellites. As reference values, Table 1 reports the $4f_{5/2}$ BE of thorium and uranium present in the metal and in the dioxide, as well as the corresponding satellite.

Fig. 2 reports U-$4f_{5/2}$ and Th-$4f_{5/2}$ core level spectra of $(U,Th)O_x$ (x < 2) thin films obtained successively by co-deposition under slight increase of oxygen partial pressure and (U,Th) metal film spectra are used as reference (red plots). It should be noted that the oxygen partial pressures used in this experiment are not universal values, but vary according to the experimental set-up. The BE and the peak shapes obtained for (U,Th) metal are in agreement with those reported in literature for single and bulk element of uranium and thorium [20,21].

The initial adding of oxygen during deposition affects first the thorium as shown by the relative increase of the *d*-screened peak whereas the uranium peak keeps constant in shape and in binding energy. The quicker oxidation of thorium relative to uranium is confirmed by the further and nearly complete oxidation of thorium (green curves) while for uranium the *f*-screened peak is still the main peak. This simple experiment demonstrates an obvious and much stronger affinity of oxygen for thorium than for uranium, as shown by the oxidation of uranium starting only once thorium is nearly completely oxidised. This is in agreement with the higher stability (lower Gibbs energy of formation) of Th^{4+} relatively to U^{4+}. The shift to lower binding energy of Th-*4f* and U-*4f* peaks is taking place due to the decrease of Fermi-energy linked to charge carrier depletion [22,23] in the sample, as reported in a previous study on ThO_2 [20]. It is a coherent shift, occurring for all photoemission lines (including O-*1s*). The thickness of the oxide layer is small enough to allow electrons to tunnel through. This avoids the charging upon photoemission and still permits a well-defined Fermi-level [24].

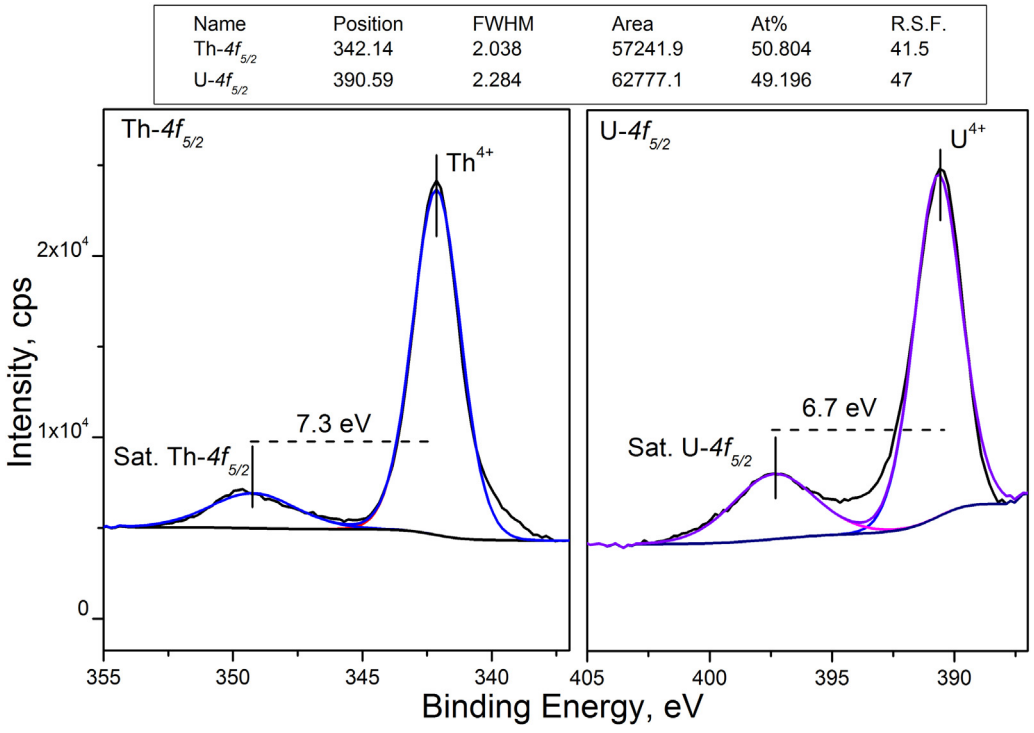

Fig. 1. Peaks Deconvolution of Th-$4f_{5/2}$ and U-$4f_{5/2}$, with peaks positions, FWHM, peaks area and quantification obtained with CasaXPS software.

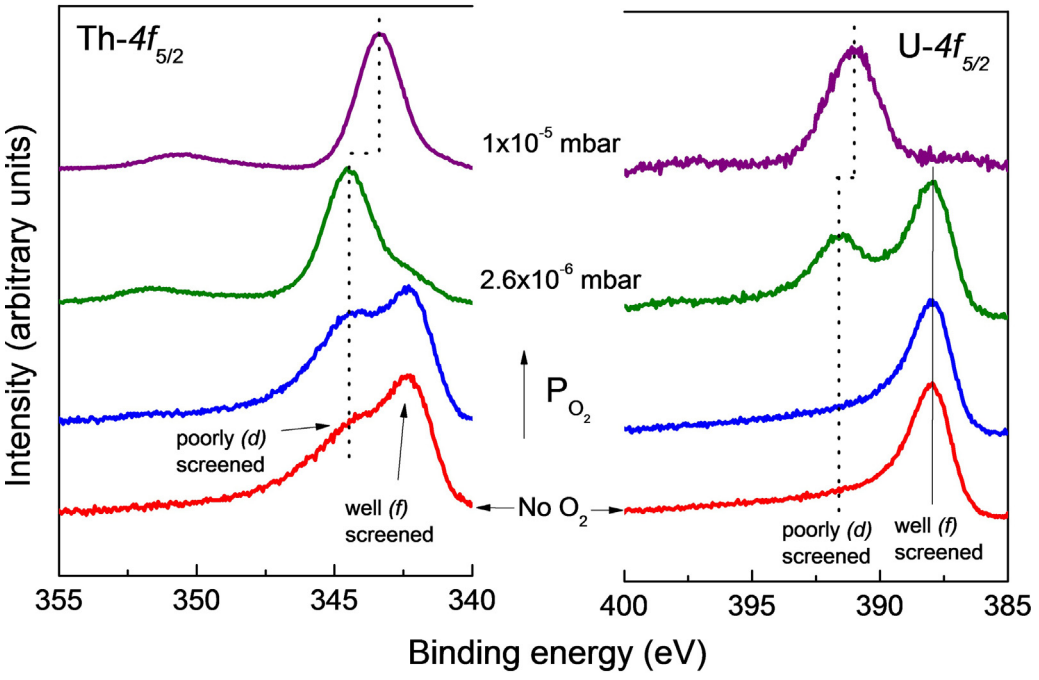

Fig. 2. Th-$4f_{7/2}$ line (left) U-$4f_{7/2}$ line (right) core level spectra for co-deposited (U,Th) films versus the relative increase of partial pressure of oxygen (PO_2).

3.2. Influence of deposition conditions and comparison with bulk data

3.2.1. Influence of deposition time and temperature on $U_{0.50}Th_{0.50}O_2$ thin films

In the following section, we compare the effect of deposition time of films at room temperature on the core level and valence band spectra. The idea behind is to investigate the reproducibility and the homogeneity of the film surface as a function of the film thickness, going from atomic to bulk properties. While XPS probes a depth of about 100 Å, XRD is looking into a sample depth of the order of a μm. Since we showed that the composition along the thickness of the film (i.e. deposition time) is constant, we consider that the composition of the surface is representative of that of the bulk.

A film composition of $U_{0.50}Th_{0.50}O_2$ has been chosen for this experiments series. The deposition rate is about 1 Å/s. Fig. 3 shows the core level spectra U-*4f* and Th-*4f* (A), the valence band (B) and

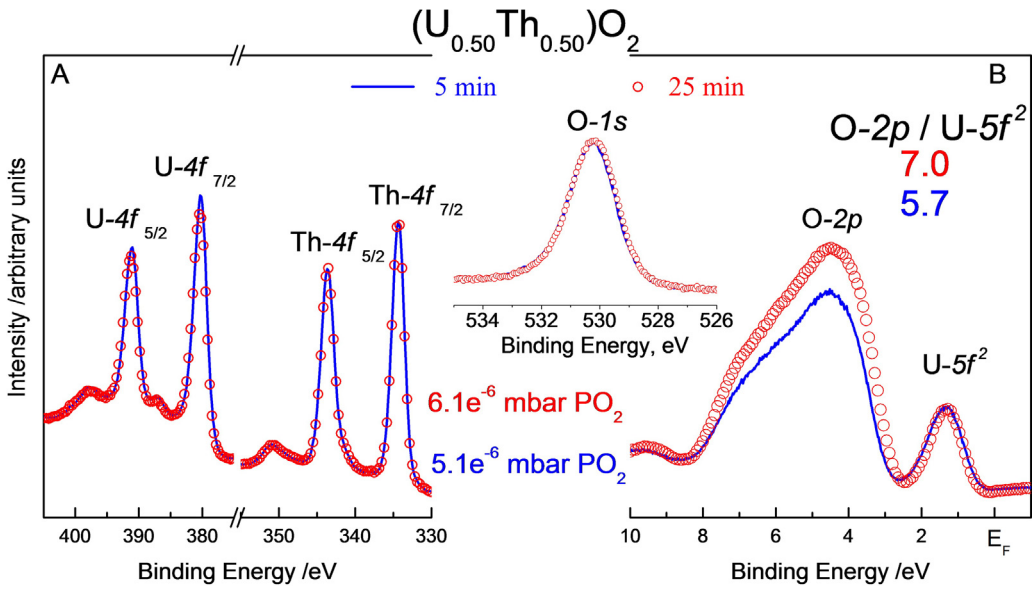

Fig. 3. The influence of the deposition time on the U-*4f* and Th-*4f* core level spectra (A) and on He*II* valence band spectra (B) for $U_{0.50}Th_{0.50}O_2$.

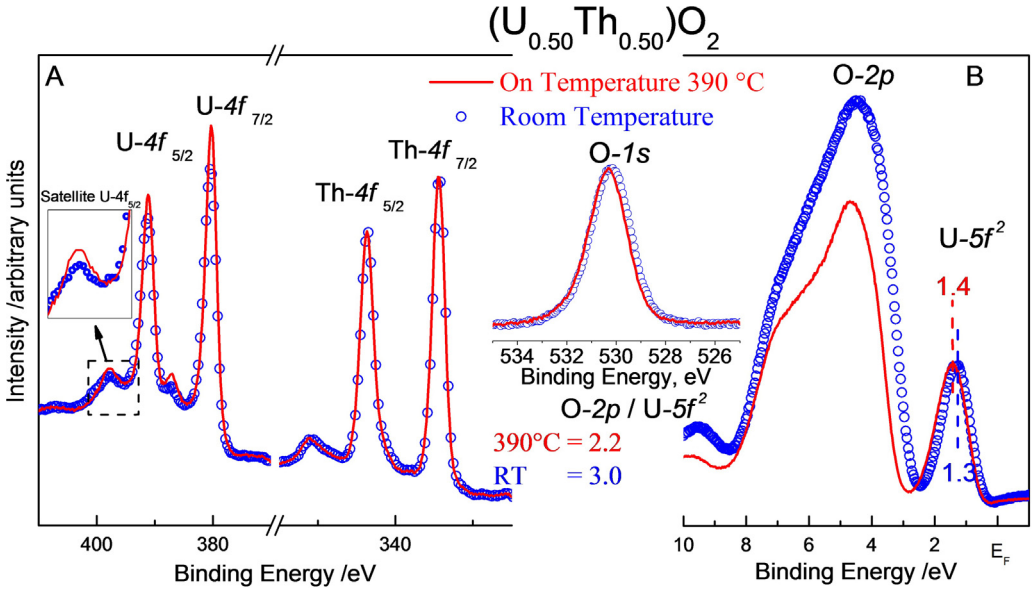

Fig. 4. The influence of the deposition temperature on the U-*4f* and Th-*4f* core level spectra (A) and on the He*II* valence band spectra (B) for a $U_{0.50}Th_{0.50}O_2$.

the corresponding O–*1s* (middle) of $U_{0.50}Th_{0.50}O_2$ film deposited during 5 min and 25 min corresponding to 30 and 150 nm, respectively. The deposition conditions were kept rigorously the same despite a small difference for the oxygen partial pressure. The Fig. 3A shows the spin-orbit splits of uranium and thorium $4f_{5/2}$ and $4f_{7/2}$. The binding energies of $4f_{7/2}$ in uranium and thorium are 380.3 eV and 334.3 eV respectively, corresponding to uranium (IV) and thorium (IV) oxidation states. The satellite peaks and the peak positions have been extensively studied in previous papers both on ThO_2 [20] and UO_2 [11]. The position and the intensity of the satellite peaks are characteristic for the oxidation states of the materials and are linked to the final state occupation. The satellite peak positions for U-Th mixed oxides (6.7 eV for U-$4f_{7/2}$ and 7.3 eV for Th-$4f_{7/2}$) are also those expected for the +IV oxidation state [25]. Within the uncertainty the quantification of the spectral lines, using CasaXPS software, does not indicate any atomic segregation at the surface for both depositions, and this is also emphasized by the constant full width at half maximum (FWHM) and binding energies. This shows the stability of the deposition technique.

The He*II* valence band spectra (Fig. 3B) are more sensitive to *5f* states compared to He*I* (not reported here) and due to the short range of the emitted photoelectrons, UPS is more sensitive to the surface than XPS. As thorium does not have a *5f* state, the peak at 1.3 eV below E_F is due to the U-$5f^2$. The peak between 3 and 9 eV is attributed to O-*2p* band emission. While XPS spectra did not show quantitative differences, UPS shows different O-*2p* band intensity and thus different ratio O-*2p*/U-*5f*, going from 5.7 to 7.0 for 5.1×10^{-6} and 6.1×10^{-6} mbar partial oxygen pressure, respectively.

With the same goal as the previous experiments, we compared the electronic structure of $U_{0.50}Th_{0.50}O_2$ films prepared with the same time of deposition at room temperature and at 390 °C. Fig. 4A reports the U-*4f* and Th-*4f* core level states and the O–*1s* spectra (inset Fig. 4), while Fig. 4B shows the corresponding He*II* valence band of $U_{0.50}Th_{0.50}O_2$. First we observed a clear superposition of the

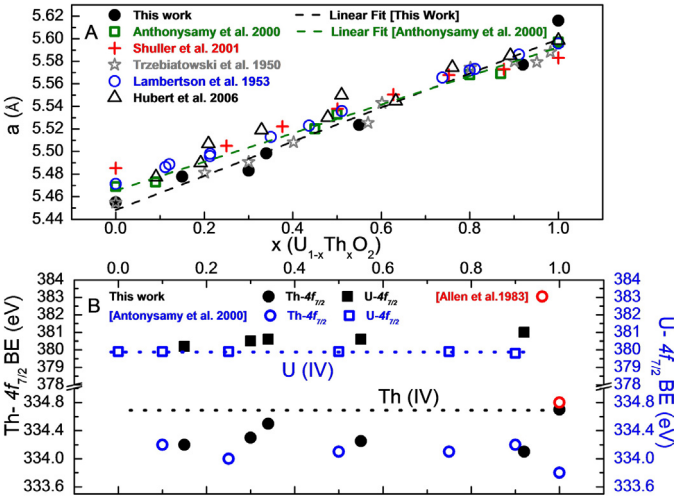

Fig. 5. Lattice parameter of $U_{1-x}Th_xO_2$ films versus x obtained in this work and compared to literature data obtained on bulk compounds (A). Th-$4f_{7/2}$ and U-$4f_{7/2}$ Binding energy in $U_{1-x}Th_xO_2$ films obtained in this work and compared to literature obtained on bulk compounds (B).

Th-*4f* core level peaks for both temperatures, while a small difference appears for the intensity of the U-*4f* peaks and for the shape of their satellites. This shows that temperature does not have an effect on the thorium states once this is completely oxidised, whereas it influences the uranium states due to the diffusion of the oxygen in the film, leading to further oxidation of U. This is also shown in the magnified satellite intensities (inset Fig. 4A) and by the slight shift towards higher BE observed in inset O–*1s* figure. The composition of the film deposited at 390 °C could be quantified as $U_{0.51}Th_{0.49}O_2$ which is within the uncertainty of the technique similar to the composition of the film deposited at room temperature. In Fig. 4B, the He*II* valence spectra show a main effect of the temperature on the O-*2p* band whose intensity and FWHM decrease, while the $5f^2$ peak shifts slightly to higher BE. The diffusion of the oxygen from the top surface to the inner of the film can explain this effect.

3.2.2. Electronic structure and lattice parameter versus composition of $U_{1-x}Th_xO_2$ films and bulk materials

To validate the use of thin films as model, we proceeded with the deposition of a series of $U_{1-x}Th_xO_2$ (x = 0 to 1) films monitoring the U-*4f* and Th-*4f* binding energies in-situ and also the lattice parameter versus the composition in ex-situ by XRD. The corresponding data reported in Fig. 5A are compared to the data obtained on bulk samples [25–29]. The lattice parameters observed for our thin films are close to the ones reported on bulk sample, following Vegard's law expected for this solid solution. The intercept of the linear fit of our work and of Anthonysamy et al. [25] study for UO_2 are 5.448 and 5.465 Å, respectively. The smaller lattice parameter found for our film can be explained by the presence of the stress in the films and with the small crystallite size as shown by the broadening of the XRD peaks [30]. Another parameter which may influence the evolution of the lattice parameter is the oxygen content which compared to bulk compounds might be slightly different from our films produced in-situ. However, XPS results showed that the films are stoichiometric.

Fig. 5B shows the BE of U-$4f_{7/2}$ and the Th-$4f_{7/2}$ in $U_{1-x}Th_xO_2$ (x = 0 to 1) versus the compositions and compares with the data obtained on bulk samples [25,31]. Vael et al. [32] pointed out that the binding energy of U-$4f_{7/2}$ for U(IV) ranges from 379.9 to 380.9 eV. Our results stay in the reported range which shows that U and Th mixed oxide are stoichiometric. Binding energies of Th-$4f_{7/2}$ are also stable in a 0.6 eV range and in a good agreement with data obtained by Allen et al. [31] but different by 1 eV relatively to the one reported by Anthonysamy et al. [25].

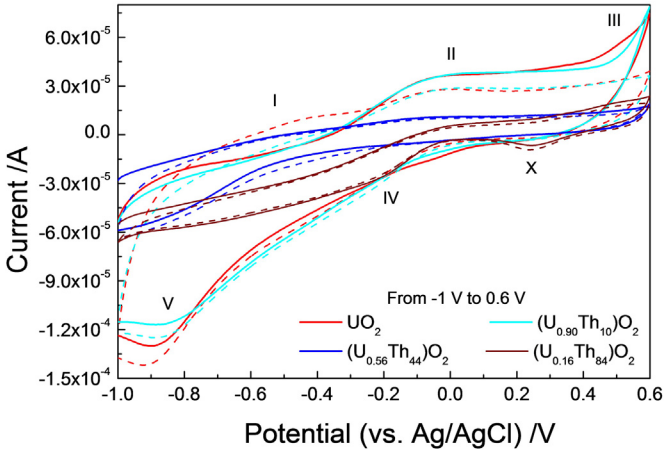

Fig. 6. Cyclic voltammetry on $U_{1-x}Th_xO_2$ (x = 0, 0.10, 0.44, 0.84, 1) films for the first two cycles.

To summarize, $U_{1-x}Th_xO_2$ (x = 0 to 1) mixed oxides films follow Vegard's law and the binding energies are in good relation with the ones obtained for bulk materials. It is apparent from these results that our thin films can be used as model for actinide oxide bulk samples, despite the microstructure which can be different (stress, preferential orientation, . . .).

3.3. Electrochemical studies

Many studies have been reported on chemical, physical properties and leaching experiments of (U,Th) mixed oxides [6,9,33,34]. Sunder et al. [9] showed that the oxidation process taking place at the surface of (U,Th) mixed oxide samples are similar to pure UO_2. However, compared to UO_2 the leaching experiments showed that the decrease of the uranium dissolution rate and this has been linked to the lower uranium content present in mixed oxide and in contact with solution. This statement has been supported by Heisbourg et al. [6,33] who studied the kinetics of dissolution of (U,Th) mixed oxides both thorium- and uranium-rich samples. Also, XPS analyses of samples obtained after leaching experiment demonstrate a surface enriched in thorium, forming a protective layer disabling further dissolution of the uranium[6]. Demkowicz et al. [34] also reported that the uranium dissolution rate in fresh samples of $(U,Th)O_2$ was 10 to 40 times lower than for conventional UO_2 fuel.

Thus compared to pure UO_2, there is a clear indication for a lower dissolution rate of uranium in (U,Th) mixed oxide, however the oxidation and reduction process is not clear yet. Sunder et al. [9] pointed out that due to the high electrical resistivity, working with electrochemical techniques on such a system as bulk material was not possible. To overcome this difficulty, thin films can be a good alternative as demonstrated by Miserque et al. [11], who reported cyclic voltammetry on UO_2 thin films. By comparing CV measurements on UO_2 thin film (1 μm) and bulk UO_2 (1 mm), it was confirmed that the films made by DC sputtering technique have much lower resistance than the bulk electrodes and the IR drop for cyclic voltammetry is negligible.

Fig. 6 shows the first two cycles of $U_{1-x}Th_xO_2$ (x = 0.10, 0.44, 0.84, 1.00) electrodes scanned between −1 V to 0.6 V (vs. Ag/AgCl) in 0.01 M NaCl. The first cycles are indicated with solid lines, the second ones are indicated with dashed lines. Roman numbers on the graphs indicate the peak positions of the suggested reactions based on literature [17,35], During the first cycle, the UO_2 electrode does not show any significant peak in region I. In this potential win-

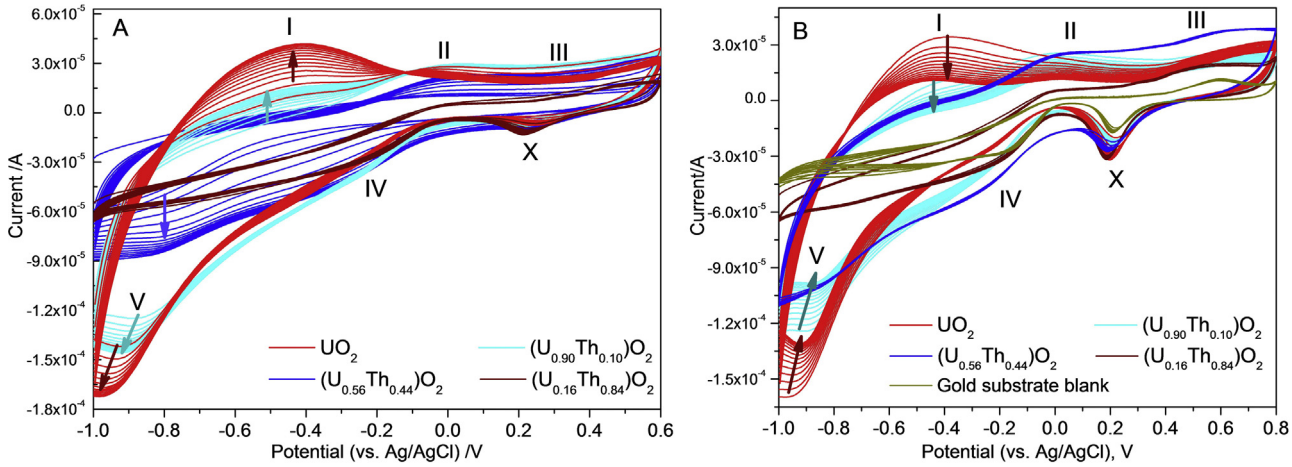

Fig. 7. Cyclic voltammetry for $U_{1-x}Th_xO_2$ (x = 0, 0.10, 0.44, 0.84, 1) films from the 3rd up to the 15th cycle in the range of −1 V to 0.6 V (A). Cyclic voltammetry for $U_{1-x}Th_xO_2$ (x = 0, 0.10, 0.44, 0.84, 1) films for higher potential window up to 0.8 V (vs. Ag/AgCl) and gold substrate cycles (yellow lines) (B). (For interpretation of the references to colour in this figure legend, the reader is referred to the web version of this article.)

dow it is thermodynamically impossible to oxidise homogeneous UO_2 and the previous studies attributed the current change to the different energy sites or inhomogeneity such as grain boundaries and hyper stoichiometry (e.g UO_{2+x}) on the surface of the electrode [17,35]. The first cycle for the UO_2, $U_{0.90}Th_{0.10}O_2$, $U_{0.56}Th_{0.44}O_2$ and $U_{0.16}Th_{0.84}O_2$ electrodes does not show any significant peaks, however, the second cycles of UO_2 and $U_{0.90}Th_{0.10}O_2$ electrodes show a slight current increase. On the other hand, at lower content of uranium (i.e. $U_{0.56}Th_{0.44}O_2$ and $U_{0.16}Th_{0.84}O_2$ electrodes) we do not observe the increase of the current, which can be explained by a lower oxidation on the surface in the first cycles.

In region II, the oxidation of UO_2 to UO_{2+x} starts and in the subsequent region III, UO_{2+x} increases to $UO_{2.33}$ by O^{2-} incorporation into the lattice. At higher potentials, the oxidation process might lead either to its dissolution as UO_2^{2+} or recrystallization as $UO_{2.5}$ and $UO_{2.66}$ (due to the adsorbed UO_2^{2+}). However, in neutral to slightly alkaline electrolytes, UO_2^{2+} in solution might re-precipitate on the electrode either as schoepite ($UO_3{\cdot}H_2O$) or as metaschoepite ($UO_3{\cdot}2H_2O$) [17,35].

In region III, a fast increase of the current is observed for both UO_2 and $U_{0.90}Th_{0.10}O_2$ electrodes indicating the onset of dissolution, which is not to such extent the case for $U_{0.56}Th_{0.44}O_2$ and $U_{0.16}Th_{0.84}O_2$ films. This process was studied by monitoring the mass loss from the UO_2 electrode in solutions of pH = 5 to pH = 8 using EQCM by Seibert et al. [12].

Region IV and V are the reduction peaks of oxidised layers observed on cathodic potentials. These peaks are usually coupled with the anodic oxidation peaks. The potentials of the peaks are related to the thickness of the oxide layer formed during the anodic scans at the surface [36]. In neutral electrolytes, region IV is observed and attributed to reduction of $UO_3{\cdot}nH_2O$ to UO_{2+x}. $UO_3{\cdot}nH_2O$ phases are insulators and thought to precipitate as porous layer and do not interfere with the reduction of the underlying oxides [37,38]. Region V is associated to the reduction of underlying oxides such as $UO_{2.33}/UO_{2+x}$ or $UO_{2.5}$, $UO_{2.67}$ created in region III, as stated above [35]. Starting from region IV and going to region V, UO_2 and $U_{0.90}Th_{0.10}O_2$ electrodes show higher cathodic currents indicating the reduction of U(VI) to U(IV). This is not the case for $U_{0.56}Th_{0.44}O_2$ and $U_{0.16}Th_{0.84}O_2$. This behaviour is also reflected in region V while UO_2 and $U_{90}Th_{10}O_2$ electrodes show reduction to stoichiometric UO_2, the other two electrodes does not indicate any compelling current activity. The low current observed at this potential window on the $U_{0.56}Th_{0.44}O_2$ and $U_{0.16}Th_{0.84}O_2$ electrodes can be attributed to the lower content of uranium in contact with the solution. Also the substitution of uranium by thorium in UO_2 lattice leads to the alteration of the electric properties (from semi-conductor UO_2 to insulator ThO_2) of mixed oxide samples. It decreases the electrical conductivity and thus the dissolution rate of uranium as reported in literature [9,39].

Fig. 7A represents the cycles from 3rd till 15th CV in the range of −1 V to 0.6 $V_{AgCl/Ag}$. In Fig. 7A, in region V, we do observe that the cathodic current increases with the uranium content. While $U_{0.90}Th_{0.10}O_2$ and, to a lesser extent, $U_{0.56}Th_{0.44}O_2$ behave in a similar way as pure UO_2, showing a shifting to higher cathodic potential along the successive cycle, $U_{0.16}Th_{0.84}O_2$ remains constant current in this region. The shifting to lower potential seems to indicate the formation of a thicker oxide layer increasing along the successive cycles (indicated with the arrows). Uncompleted reduction in domain V leads to an increase of oxidation on region I of the current getting higher and higher in each cycle. The same phenomenon is not observed for $U_{0.56}Th_{0.44}O_2$ and $U_{0.16}Th_{0.84}O_2$ electrodes due to the lower amount of uranium. In region II and III, where oxidation of UO_2 and UO_{2+x} is taking place, the current increases with the content of the uranium present in the electrodes.

When the scans continued up to 0.8 $V_{Ag/AgCl}$ for another 15 cycles, differences were observed as shown in Fig. 7B. Looking at the peaks in region V and region I, we do observe an opposite trend compared to Fig. 7A. The broader scan window to higher anodic potential leads a shifting to lower cathodic potential of region V and to a decrease of current along the cycles in regions V and I. This might be due to fact that higher dissolution rates are achieved at higher anodic potentials. This decrease in intensity of peaks in region V and I may be related to the decrease of the thickness of the hyperstoichiometric oxide layers (region V), thus leading to less different energy sites or grain boundaries on the surface (region I). The reason why this is happening in this bigger potential window is not totally clear.

Gold used as substrate and considered as noble metal does not interfere strongly in the working potential window chosen in this study, as shown in Fig. 7B in yellow lines. In the potential windows up to 0.6 V (not reported here) it has no effect as demonstrated by the low current value, but when measured up to 0.8 V a peak marked as X on the cathodic potentials is observed. This might be attributed to the electrolyte reduction. The films have a certain porosity enabling the contact of the solution with gold substrate. The intensity peak X increase along the successive cycles and can be related to the oxide layer getting more and more porous while the gold surface increases together with its related current.

Table 2
Composition and U-4f$_{5/2}$, Th-4f$_{5/2}$ and O–1s of films before and after 30 cycles of CV in [NaCl] = 0.01 M.

Sample	Before CV				After CV			
	Composition	Binding Energy, eV			Composition	Binding Energy, eV		
		U-$4f_{5/2}$	Th-$4f_{5/2}$	O-*1s*		U-$4f_{5/2}$	Th-$4f_{5/2}$	O-*1s*
1	$U_{0.67}Th_{0.33}O_2$	380.5	334.0	529.8	$U_{0.57}Th_{0.43}O_{2+x}$	381.3	334.1	529.7/531.2
2	$U_{0.56}Th_{0.44}O_2$	380.5	333.9	529.8	$U_{0.40}Th_{0.60}O_{2+x}$	381	333.9	529.8/531.2
3	$U_{0.16}Th_{0.84}O_2$	380.5	333.9	529.8	$U_{0.14}Th_{0.86}O_{2+x}$	380.9	333.8	529.7/531.3

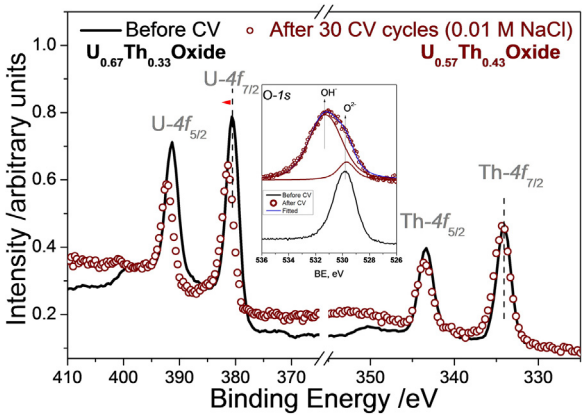

Fig. 8. U-*4f* and Th-*4f* of $U_{0.67}Th_{0.33}$ oxide film before and after 15 cycles, inset graph represents the corresponding O–*1s* spectra.

The current counts for the $U_{0.56}Th_{0.44}O_2$ and $U_{0.16}Th_{0.84}O_2$ electrodes throughout their consecutive CVs have about the same values, which can be explained by the lower amount of uranium at the surface. The $U_{0.16}Th_{0.84}O_2$ electrode is rather behaving as the gold substrate itself. It has a higher current than gold substrate due to the small amount of uranium on the surface. Nonetheless the current activity should be related to the electrolyte interference because Thorium is not expected to show any oxidation on these potential window [40].

Fig. 8 compares the U-*4f* and Th-*4f* spectra of $U_{0.67}Th_{0.33}O_2$ film obtained before and after CV as an example the general observations. First the U-*4f* peaks shift to higher binding energy indicating further oxidation as UO_{2+x}, unlike the Th-*4f* peaks that keep a constant binding energy because no further oxidation than Th(IV) can take place. We also observed the change in the intensity peaks. When the two spectra before and after the CV experiment are normalized to Th-*4f*, the U-*4f* intensity peaks decreased after the CV cycles, indicating a lower uranium content at the surface compared to the initial, as deposited film composition. Also the shift of U-4f to higher binding energy after CV experiment indicates a higher oxidation state for uranium at the surface. The quantification using CasaXPS shows that the composition changes from $U_{0.67}Th_{0.33}O_2$ to $U_{0.57}Th_{0.43}O_{2+x}$. In the inset of Fig. 8 we observe the broadening of the peak O–*1s* which can be deconvoluted in two components, at low BE and one at higher BE, corresponding to O^{2-} and to OH^- respectively [33,41]. The O–*1s* shift is more pronounced on the films that contain higher amount of uranium on the composition.

To summarize the CV experiment on the mixed oxide films, Table 2 reports the compositions and the BE of U-$4f_{5/2}$, Th-$4f_{5/2}$ and O–*1s* core level peaks for the different samples before and after CV cycles. The results show a strong decrease of uranium content relative to thorium, decreasing by about 30 at% (sample 2) compared to the initial composition. The preferential dissolution of uranium at the surface enables to explain this result leading to an enrichment of thorium at the surface which along oxidation and dissolution of U(VI) provides a protection layer inhibiting the further oxidation of the uranium present deeper in the film. The thorium effect has been discussed in literature [6,9,33] reporting its role to passivate the surface, limiting further oxidation of uranium and decreasing the dissolution rate of uranium. Our results enable to confirm this process taking place at the surface of the sample in contact with a neutral solution.

4. Conclusion and summary

Thin films of $U_{1-x}Th_xO_2$ (x = 0 to 1) mixed oxides were investigated by XPS/UPS, XRD and CV to establish the possible influence of thorium on the oxidation/dissolution process.

We first investigated the relative oxygen affinity of Th and U and oxidation of uranium started only once thorium was completely oxidized. This observation is consistent with the higher stability of ThO_2 (Δ_fG^0 (298 K): −1170 kJ mol^{-1}) compared to UO_2 (Δ_fG^0 (298 K): −1031 kJ mol^{-1} [42]).

Based on core level and valence band spectra, homogeneity of the films could be showed along the deposition. Also deposition temperature (from 25 °C to about 400 °C) had no influence on thorium oxidation state while uranium undergoes further oxidation, seen by a shift of the U-*4f* satellite and the U-$5f^2$ peak, and by a change of the O-*2p*/U-$5f^2$ intensity ratio.

To determine the suitability of thin films as model system for nuclear fuel we compared the lattice parameters and the U-*4f* and Th-*4f* core level binding energy of films to bulk compounds, for a series of compositions of $U_{1-x}Th_xO_2$ (x = 0 to 1). The lattice parameters followed the Vegardís law, with a slight deviation attributed to stress present in the films. Also the binding energies of U-*4f* and Th-*4f* core levels were in agreement with those reported on bulk compounds.

Cyclic voltammetry was used to follow the surface redox reactions for different compositions. In the potential window of [−1 to 0.6] V (vs Ag/AgCl), oxidative dissolution of uranium in neutral pH solution suggests the formation of a layer of higher oxide at the surface. Shift of the peaks to the higher negative potentials are observed in the cathodic region V at about −0.9 V (vs Ag/AgCl), as well as in current intensity increase in the anodic region at about −0.5 V (vs Ag/AgCl) in region I, indicating formation of thicker layers hyperstoichiometric oxides on each cycle performed. The intensity and the position of the peaks showed a proportional relation with the thorium content in UO_2 matrix. However, on a larger potential window [-1 to 0.8] V (vs Ag/AgCl), an opposite behaviour is observed, such as lower intensity and adverse direction shifts on each cycles. This change in behaviour showed that the successive cycles result in thinner layers of hyperstoichiometric oxides on the surface. On the other hand, in the higher potential window we observed higher current counts for both anodic and cathodic potentials for films with higher thorium content (going from $U_{0.56}Th_{0.44}O_2$ and $U_{0.16}Th_{0.84}O_2$). This can be explained by the fact that a higher thorium concentration requires higher potentials to oxidise uranium.

The XPS spectra obtained on samples, before and after CV experiments, indicated clearly enrichment in thorium at the surface and a higher oxidation state of uranium. The results also indicated that a higher initial uranium content on the surface leads to a higher

shift of U-*4f* binding energies, suggesting a higher oxidation state of uranium. This was supported by the shape of the corresponding O–*1s* spectrum showing higher contribution of oxygen from OH^- groups.

Acknowledgments

We thank D. Wegen and A. Seibert for fruitful discussions and also to S. Stumpf and Z. Bao for the XRD measurements. P. Cakir acknowledges the European Commission and Joint Research Centre.

References

[1] Y. Lu, Y. Yang, P. Zhang, Thermodynamic properties and structural stability of thorium dioxide, J. Phys. Condens. Matter 24 (2012) 225801, http://dx.doi.org/10.1088/0953-8984/24/22/225801.
[2] J.S. Herring, P.E. MacDonald, K.D. Weaver, C. Kullberg, Low cost, proliferation resistant, uranium-thorium dioxide fuels for light water reactors, Nucl. Eng. Des. 203 (2001) 65–85, http://dx.doi.org/10.1016/s0029-5493(00)00297-1.
[3] I. Grenthe, J. Fuger, R.J.M. Konings, R.J. Lemire, A.G. Muller, C. Nguyen-Trung Cregu, et al. Chemical thermodynamics of uranium, North Holland Amsterdam (1992).
[4] D. Langmuir, J.S. Herman, The Mobility of Thorium in Natural Waters at low Temperatures, Geochim. Cosmochim. Acta 44 (1980) 1753–1766.
[5] A. Seibert, S. Stumpf, T. Gouder, D. Schild, M.A. Denecke, Actinide thin films as surface models, in: Actin. Nanoparticle Res., Springer Berlin Heidelberg, Berlin, Heidelberg, 2011, pp. 275–313, http://dx.doi.org/10.1007/978-3-642-11432-8_10.
[6] G. Heisbourg, S. Hubert, N. Dacheux, J. Ritt, The kinetics of dissolution of Th1-xUxO2 solid solutions in nitric media, J. Nucl. Mater. 321 (2003) 141–151, http://dx.doi.org/10.1016/S0022-3115(03)00213-7.
[7] E. Zimmer, E. Merz, Dissolution of thorium-uranium mixed oxides in concentrated nitric acid, J. Nucl. Mater. 124 (1984) 64–67, http://dx.doi.org/10.1016/0022-3115(84)90010-2.
[8] R. Rao, R.K. Bhagat, N.P. Salke, A. Kumar, Raman spectroscopic investigation of thorium dioxide-uranium dioxide (ThO2-UO2) fuel materials, Appl. Spectrosc. 68 (2014) 44–48, http://dx.doi.org/10.1366/13-07172.
[9] S. Sunder, N.H. Miller, XPS and XRD studies of (Th,U)O2 fuel corrosion in water, J. Nucl. Mater. 279 (2000) 118–126, http://dx.doi.org/10.1016/S0022-3115(99)00242-1.
[10] C.A. Colmenares, The oxidation of thorium uranium, and plutonium, Prog. Solid State Chem. 9 (1975) 139–239.
[11] F. Miserque, T. Gouder, D.H. Wegen, P.D.W. Bottomley, Use of UO2 films for electrochemical studies, J. Nucl. Mater. 298 (2001) 280–290.
[12] A. Seibert, D.H. Wegen, T. Gouder, J. Römer, T. Wiss, J.-P. Glatz, The use of the electrochemical quartz crystal microbalance (EQCM) in corrosion studies of UO2 thin film models, J. Nucl. Mater. 419 (2011) 112–121, http://dx.doi.org/10.1016/j.jnucmat.2011.06.032.
[13] D.W. Shoesmith, Fuel corrosion processes under waste disposal conditions, J. Nucl. Mater. 282 (2000) 1–31, http://dx.doi.org/10.1016/S0022-3115(00)00392-5.
[14] L. Wu, Z. Qin, D.W. Shoesmith, An improved model for the corrosion of used nuclear fuel inside a failed waste container under permanent disposal conditions, Corros. Sci. 84 (2014) 85–95, http://dx.doi.org/10.1016/j.corsci.2014.03.019.
[15] S. Sunder, N.H. Miller, D.W. Shoesmith, Corrosion of uranium dioxide in hydrogen peroxide solutions, Corros. Sci. 46 (2004) 1095–1111, http://dx.doi.org/10.1016/j.corsci.2003.09.005.
[16] S. Sunder, D.W. Shoesmith, R.J. Lemire, M.G. Bailey, G. j. Wallace, The effect of pH on the corrosion of nuclear fuel (UO2) in oxygenated solutions, Corros. Sci. 32 (1991) 373–386.
[17] S. Sunder, D.W. Shoesmith, M.G. Bailey, F.W. Stanchell, N.S. McIntyre, Anodic oxidation of UO2 Part I. Electrochemical and X-Ray photoelectron spectroscopic studies in neutral solutions, J. Electroanal. Chem. 130 (1981) 163–179.
[18] D.W. Shoesmith, S. Sunder, The prediction of nuclear fuel (UO2) under waste disposal conditions, J. Nucl. Mater. 190 (1992) 20–35.
[19] N. Fairley, CASA XPS Manual 2.3.15 Introduction to XPS and AES, (2009) 1–177.
[20] P. Cakir, R. Eloirdi, F. Huber, R.J.M. Konings, T. Gouder, An XPS and UPS study on the electronic structure of ThO x ($x \leq 2$) thin films, J. Phys. Chem. C 118 (2014) 24497–24503.
[21] J.J. Pireaux, J. Riga, E. Thibaut, C. Tenret-Noel, Shake-up satellites in the X-ray photoelectron spectra of uranium oxides and fluorides. A band structure scheme for uranium dioxides, UO2, Chem. Phys. 22 (1977) 113–120.
[22] A. Cros, Charging effects in X-ray photoelectron, J. Electron Spectrosc. Relat. Phenom. 59 (1992) 1–14.
[23] J. Cazaux, Mechanisms of charging in electron spectroscopy, J. Electron Spectrosc. Relat. Phenom. 105 (1999) 155–185, http://dx.doi.org/10.1016/S0368-2048(99)00068-7.
[24] G. Fanjoux, H. Fornander Billault, B. Lescop, a. Le Nadan, Evolution of the magnesium surface during oxidation studied by Metastable Impact Electron Spectroscopy, J. Electron Spectrosc. Relat. Phenom. 119 (2001) 57–67, http://dx.doi.org/10.1016/S0368-2048(01)00237-7.
[25] S. Anthonysamy, G. Panneerselvam, S. Bera, S.V. Narasimhan, P.R. Vasudeva Rao, Studies on thermal expansion and XPS of urania-thoria solid solutions, J. Nucl. Mater. 281 (2000) 15–21, http://dx.doi.org/10.1016/s0022-3115(00)00185-9.
[26] L.C. Shuller, R.C. Ewing, U. Becker, Thermodynamic properties of ThxU1-xO2 ($0 < x < 1$) based on quantum-mechanical calculations and Monte-Carlo simulations, J. Nucl. Mater. 412 (2011) 13–21, http://dx.doi.org/10.1016/j.jnucmat.2011.01.017.
[27] W. Trzebiatowski, P.W. Selwood, Magnetic susceptibilities of urania-thoria solid solutions, J. Am. Chem. Soc. 72 (1950) 4504–4506, http://dx.doi.org/10.1021/ja01166a046.
[28] W.A. Lambertson, M.H. Mueller, F.H. Gunzel, Uranium oxide phase equilibrium systems: IV, UO2-ThO2, J. Am. Ceram. Soc. 36 (1953) 397–399, http://dx.doi.org/10.1111/j.1151-2916.1953.tb12827.x.
[29] S. Hubert, J. Purans, G. Heisbourg, P. Moisy, N. Dacheux, Local structure of actinide dioxide solid solutions Th(1-x)U(x)O2 and Th(1-x)Pu(x)O2, Inorg. Chem. 45 (2006) 3887–3894, http://dx.doi.org/10.1021/ic050888y.
[30] M.M. Strehle, B.J. Heuser, M.S. Elbakhshwan, X. Han, D.J. Gennardo, H.K. Pappas, et al., Characterization of single crystal uranium-oxide thin films grown via reactive-gas magnetron sputtering on yttria-stabilized zirconia and sapphire, Thin Solid Films 520 (2012) 5616–5626, http://dx.doi.org/10.1016/j.tsf.2012.04.022.
[31] G.C. Allen, P.M. Tucker, J.W. Tyler, Electronic structure of some binary uranium and thorium oxides and halides, Philos. Mag. Part B 48 (1983) 63–75, http://dx.doi.org/10.1080/13642818308226432.
[32] B.W. Veal, D.J. Lam, H. Diamond, H.R. Hoekstra, X-ray photoelectron-spectroscopy study of oxides of the transuranium elements Np, Pu Am, Cm, Bk, and Cf, Phys. Rev. B 15 (1977) 2929–2942.
[33] G. Heisbourg, S. Hubert, N. Dacheux, J. Purans, Kinetic and thermodynamic studies of the dissolution of thoria-urania solid solutions, J. Nucl. Mater. 335 (2004) 5–13, http://dx.doi.org/10.1016/j.jnucmat.2004.05.017.
[34] P.A. Demkowicz, J.L. Jerden, J.C. Cunnane, N. Shibuya, R. Baney, J. Tulenko, Aqueous dissolution of urania/thoria nuclear fuel, Nucl. Technol. 147 (2004) 157–170.
[35] D.W. Shoesmith, S. Sunder, W.H. Hocking, Electrochemistry of UO2 nuclear fuel, in: J. Lipkowski, N.P. Ross (Eds.), Electrochem. Nov. Mater., VCH, New York, 1994, pp. 297–337.
[36] B.G. Santos, J.J. Noël, D.W. Shoesmith, The effect of pH on the anodic dissolution of SIMFUEL (UO2), J. Electroanal. Chem. 586 (2006) 1–11, http://dx.doi.org/10.1016/j.jelechem.2005.09.021.
[37] B. Santos, H. Nesbitt, J. Noël, D. Shoesmith, X-ray photoelectron spectroscopy study of anodically oxidized SIMFUEL surfaces, Electrochim. Acta 49 (2004) 1863–1873, http://dx.doi.org/10.1016/j.electacta.2003.12.016.
[38] S. Sunder, L.K. Strandlund, D.W. Shoesmith, Anodic oxidation and dissolution of CANDU fuel (UO2) in slightly alkaline sodium perchlorate solutions, Electrochim. Acta 43 (1998) 2359–2372, http://dx.doi.org/10.1016/S0013-4686(97)10174-8.
[39] D.E. Grandstaff, A kinetic study of the dissolution of uraninite, Econ. Geol. 71 (1976) 1493–1506, http://dx.doi.org/10.2113/gsecongeo.71.8.1493.
[40] B. Kanellakopulus, General properties of thorium atom and thorium ions, in: R.J. Meyer (Ed.), Gmelin Handb. Inorg. Chem. Thorium, 8th ed., Springer-Verlag, Berlin, Heidelberg, New York, Tokyo, 1989, pp. 1–17.
[41] J.-C. Dupin, D. Gonbeau, P. Vinatier, A. Levasseur, Systematic XPS studies of metal oxides, hydroxides and peroxides, Phys. Chem. Chem. Phys. 2 (2000) 1319–1324, http://dx.doi.org/10.1039/a908800h.
[42] R. Agarwal, S.C. Parida, Phase diagrams and thermodynamic properties of thoria, thoria–urania, and thoria–plutonia, in: D. Das, S.R. Bharadwaj (Eds.), Thoria-Based Nucl. Fuels, Green Energy Technol., Springer-Verlag, London, 2013, pp. 71–105, http://dx.doi.org/10.1007/978-1-4471-5589-8_3.
[43] J.C. Fuggle, M. Campagna, Z. Zolnierek, R. Lässer, A. Platau, Observation of a relationship between core-level line shapes in photoelectron spectroscopy and the localization of screening orbitals, Phys. Rev. Lett. 45 (1980) 1597–1600, http://dx.doi.org/10.1103/PhysRevLett.45.1597.
[44] J.C. Fuggle, A.F. Burr, L.M. Watson, D.J. Fabian, W. Lang, X-ray photoelectron studies of thorium and uranium, J. Phys. F Met. Phys. 4 (1974) 335.
[45] M.O. Krause, R.G. Haire, O. Keski-Rahkonen, J.R. Peterson, Photoelectron spectrometry of the actinides from Ac to Es, J. Electron Spectrosc. Relat. Phenom. 47 (1988) 215–226, http://dx.doi.org/10.1016/0368-2048(88)85013-8.
[46] G.C. Allen, J.A. Crofts, M.T. Curtis, P.M. Tucker, D. Chadwick, J.P. Hampson, X-Ray photoelectron spectroscopy of some uranium oxide phases, J. Chem. Soc. Dalton Trans. 129 (1974) 6–130 (1).